Intumescent ethylene-vinyl acetate copolymer: Reaction to fire and mechanistic aspects

Serge Bourbigot, Johan Sarazin, Fabienne Samyn, Maude Jimenez

▶ **To cite this version:**

Serge Bourbigot, Johan Sarazin, Fabienne Samyn, Maude Jimenez. Intumescent ethylene-vinyl acetate copolymer: Reaction to fire and mechanistic aspects. Polymer Degradation and Stability, 2019, Polymer Degradation and Stability, pp.235-244. 10.1016/j.polymdegradstab.2019.01.029 . hal-02075670

HAL Id: hal-02075670
https://hal.univ-lille.fr/hal-02075670v1

Submitted on 21 Mar 2019

HAL is a multi-disciplinary open access archive for the deposit and dissemination of scientific research documents, whether they are published or not. The documents may come from teaching and research institutions in France or abroad, or from public or private research centers.

L'archive ouverte pluridisciplinaire **HAL**, est destinée au dépôt et à la diffusion de documents scientifiques de niveau recherche, publiés ou non, émanant des établissements d'enseignement et de recherche français ou étrangers, des laboratoires publics ou privés.

Accepted Manuscript

Intumescent ethylene-vinyl acetate copolymer: Reaction to fire and mechanistic aspects

Serge Bourbigot, Johan Sarazin, Fabienne Samyn, Maude Jimenez

PII: S0141-3910(19)30037-0

DOI: https://doi.org/10.1016/j.polymdegradstab.2019.01.029

Reference: PDST 8768

To appear in: *Polymer Degradation and Stability*

Received Date: 26 October 2018

Revised Date: 24 January 2019

Accepted Date: 25 January 2019

Please cite this article as: Bourbigot S, Sarazin J, Samyn F, Jimenez M, Intumescent ethylene-vinyl acetate copolymer: Reaction to fire and mechanistic aspects, *Polymer Degradation and Stability* (2019), doi: https://doi.org/10.1016/j.polymdegradstab.2019.01.029.

This is a PDF file of an unedited manuscript that has been accepted for publication. As a service to our customers we are providing this early version of the manuscript. The manuscript will undergo copyediting, typesetting, and review of the resulting proof before it is published in its final form. Please note that during the production process errors may be discovered which could affect the content, and all legal disclaimers that apply to the journal pertain.

ACCEPTED MANUSCRIPT

Intumescent ethylene-vinyl acetate copolymer: reaction to fire and mechanistic aspects

Serge Bourbigot*[1], Johan Sarazin[1], Fabienne Samyn[1] and Maude Jimenez[1]

[1] *R_2Fire group/UMET – UMR CNRS 8207, ENSCL, University of Lille, France*

Corresponding author: serge.bourbigot@ensc-lille.fr

ABSTRACT

The concept of intumescence was applied to flame retard ethylene vinyl acetate copolymer (EVA). The paper examines two types of intumescence based on expandable graphite (EG, physical expansion) and on modified ammonium polyphosphate (AP760, chemical expansion). The incorporation of expandable graphite (EG) at relatively low loading (10 wt%) in EVA permits the reduction up to 65% of peak of heat release rate (pHRR) measured by cone calorimetry. The mode of action occurs via the formation of an expanded carbonaceous layer acting mainly as heat barrier limiting heat and mass transfer as evidenced by the temperature measurement as a function of time during cone calorimetry. The incorporation of small amount of $ZnCO_3$ in EVA-AP760 enhances strongly the performance: pHRR was not reduced using the sole AP760 while it is decreased by 54% when only 2 wt% of AP760 is substituted by $ZnCO_3$. A strong synergistic effect was therefore observed. Solid state NMR of ^{31}P and ^{13}C on cone residues prepared at different characteristic times evidenced the mechanism involved is the reinforcement of the protective char by the formation of phosphate glass limiting the creation of cracks and increasing the char strength.

KEYWORDS:

Intumescence; ethylene-vinyl acetate copolymer; expandable graphite; fire chemistry; synergy, solid state NMR

INTRODUCTION

Ethylene-vinyl acetate copolymer (EVA) is a material that combines flexibility and strength and has many potential applications in packaging and manufacturing [1]. Those copolymers are used extensively in the wire and cable industry for making heat shrinkable insulation, semi-conductive insulation jackets, and flame retardant insulation. Aluminum trihydroxide (ATH) as flame-retardant (FR) is usually incorporated in EVA at content around 50–70 wt.% to achieve a satisfactory degree of flame retardancy [2]. However this loading can dramatically change of the mechanical properties of the material and leads to processing issues. The motivation of this paper is to examine the flame retardancy of EVA using the concept of intumescence.

When heated beyond a critical temperature, an intumescent material begins to swell and then to expand. The result of this process is a foamed cellular charred layer on the surface, which protects the underlying material from the action of the heat flux or the flame. Visually, the swelling looks like ‘black waves’ swollen at the surface of the material and the final char exhibits hemispheric

ACCEPTED MANUSCRIPT

shape with a roughed or smooth surface. The concept of intumescence enables to make flame retarded polymeric materials (including EVA-based materials) exhibiting high performance [3-6]. This paper examines two types of intumescence in EVA based on expandable graphite (EG, physical expansion) and on modified ammonium polyphosphate (AP760, chemical expansion). Some examples of using ammonium polyphosphate and expandable graphite can be found elsewhere [7-9]. Reaction to fire of EVA containing EG and AP760 is first evaluated by cone calorimetry and the efficiency of the intumescent barrier is measured at the same time. The results are compared to a conventional flame retarded EVA using ATH as flame retardant. Based on the fire behavior of certain intumescent EVA, synergist was also evaluated and the results associated with a mechanism of action are presented in the last part of the paper.

EXPERIMENTAL

Materials and processing

Commercial grade of EVA was used in this work: the Evatane 28-05 supplied by Arkema (France). It exhibits a melt flow index in the range at 190°C (2.16 kg) of 5-8 g/10 min and a melting point of 72°C. This grade of EVA contains 28% vinyl acetate.

Expandable graphite (EG) is the commercial grade ES350F5 from Graphitwerk Kropfmühl (Germany) with an average particle size of 300 µm. EG is a synthesized intercalation compound of graphite that expands or exfoliates when heated. A wide variety of chemical species can be used to intercalate graphite materials (e.g. sulfate, nitrate, various organic acids …) [10]. Sulfate was used in this grade to make graphite bisulfate. Modified ammonium polyphosphate (AP760) is the commercial grade of Clariant (Germany) with the brand name Exolit AP760. It is an intrinsic intumescent system containing 20 wt% phosphorus and 14 wt% nitrogen acting in synergy. It is mainly based on ammonium polyphosphate as acid source and tris(hydroxyethyl) isocyanurate (THEIC) as char former. Aluminum trihydroxide (ATH) is widely used for the flame retardancy of EVA and it was evaluated for comparison with the intumescent systems. It was supplied in white powder (D_{50} = 1.3 µm) under the brand name Apyral 40CD by Nabaltec (Schwandorf, Germany). Zinc carbonate was supplied by Sigma-Aldrich (CAS Number 5263-02-5) and was used as substituting ingredient.

ACCEPTED MANUSCRIPT

Processing

The strategy was to blend EVA with the flame-retardants (FRs) described above using HAAKE Rheomix OS PTW 16 twin-screw extruder. The extruder is a co-rotating intermeshing twin screw with a barrel length of 400 mm and screw diameter of 16 mm (L/D = 25) with 10 heating zones. EVA and FRs were incorporated using two gravimetric side feeders into the extruder. Polymer flow rate is fixed to extrude about 500 g/h with a screw speed of 250 rpm. The temperature profile from feeder to die was set at 150/ 160/ 160/ 170/ 170/ 170/ 160/ 160/ 160/ 150°C.

The total loading of intumescent FRs in EVA was 10 wt% varying the ratio AP760/EG (wt/wt) at 10:0; 5:5; and 0:10. This loading was selected because it provides an acceptable performance according to cone calorimetry. The purpose was also to evaluate the fire behavior of the materials at relatively low loading. Note ATH was incorporated at 65 wt% in EVA because it is the usual loading with this filler. Compounding was performed with the same equipment and the same conditions as described above.

Cone calorimetry

FTT (Fire Testing Technology) Mass Loss Calorimeter (MLC) was used to carry out measurements on samples following the procedure defined in ASTM E 906. The equipment is identical to that used in oxygen consumption cone calorimetry (ASTM E-1354-90), except that a thermopile in the chimney is used to obtain heat release rate (HRR) rather than employing the oxygen consumption principle. Our procedure involved exposing specimens measuring 100 mm x 100 mm x 3 mm in horizontal orientation. External heat flux of 35 kW/m² was used for running the experiments (distance of 35 mm between the sample and the cone heater). This flux corresponds to common heat flux in mild fire scenario. MLC was used to determine heat release rate (HRR). When measured at 35 kW/m², HRR is reproducible to within ±10%. The cone data reported in this paper are the average of three replicated experiments.

In addition to those measurements, a thermocouple was embedded on the backside of the materials in horizontal position. They measured temperature as a function of time during a regular cone experiment. In this experimental set-up, it is necessary to assume that additional conductive effects due to the thermocouple are negligible.

ACCEPTED MANUSCRIPT

Solid state NMR

^{31}P NMR experiments were performed on a 9.4 T Bruker Avance spectrometer operating at 162 MHz. Ground samples were packed in 4-mm fused zirconia rotors and sealed with Kel-F caps. The analysis was carried out with a 4 mm probehead with ^{1}H decoupling. The spectrum was recorded at magic angle spinning (MAS) with a spinning frequency of ν_{rot} = 12.5 kHz, a 2 µs pulse length (corresponding to a $\pi/2$ flip angle) a rd of 120 s and 16 transients. The ^{31}P chemical shift was referred to H_3PO_4 at 0 ppm.

^{13}C NMR experiment was conducted on the same spectrometer as above operating at 100.6 MHz, at ν_{rot} = 10 kHz with a 4 ms pulse length (corresponding to a $\pi/2$ flip angle), a rd of 10 s and 4096 transients. High-power ^{1}H decoupling and ^{1}H-^{13}C cross-polarization (CP) were used (acquisition with a contact time of 1 ms). The ^{13}C chemical shift was referred to tetramethylsilane at 0 ppm.

Mechanical resistance of intumescent char

Mechanical resistance of intumescent char was measured according to a novel protocol developed in our lab [11]. Rheological measurements were carried out using a Rheometric Scientific ARES-20A Thermal Scanning Rheometer (TSR) in a parallel plate configuration. Mechanical resistance is evaluated using the protocol described as follows: at t=0 s, the sample (height, h=1 mm) is put into the furnace and heated to 500 °C without applying any strain (the upper plate is not in contact with the sample as shown in Fig. 2). This allows the sample to intumesce without any constraint. Keeping the temperature at 500°C, the upper plate is then brought into contact with the intumesced material and the separation between the plates is reduced linearly (0.02 mm/s). The force is followed as a function of the separation between the two plates (Fig. 2). The upper plate used in this experiment has a diameter of 5 mm in order to increase the pressure on the whole sample and to ensure complete destruction of the char. Note there is no oscillation of the plate during the test.

ACCEPTED MANUSCRIPT

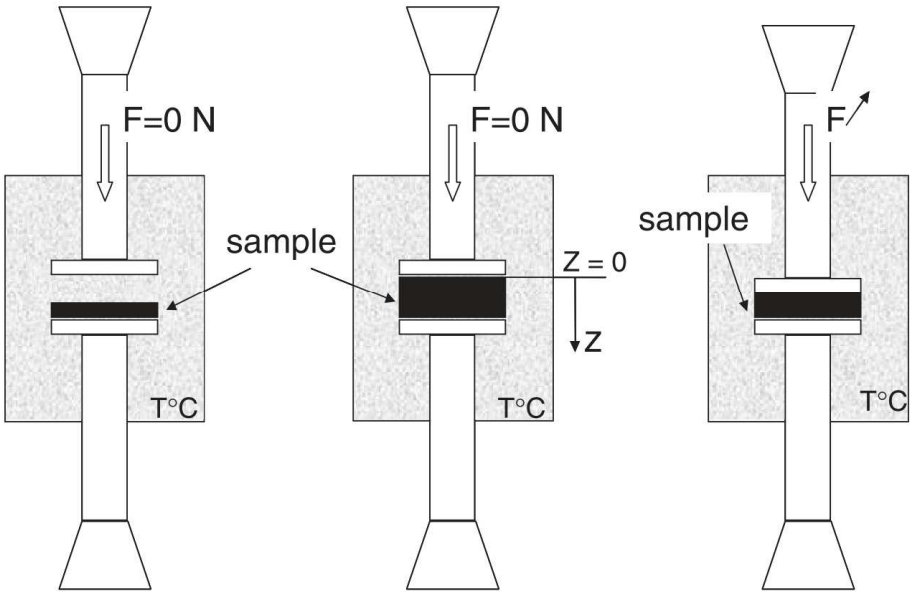

Fig. 1. Scheme of the measurement of the mechanical resistance of intumescent char (adapted from [11])

RESULTS AND DISCUSSION

Reaction to fire of intumescent EVA

EG and AP760 and their combination (AP760/EG at 5:5 (wt/wt)) were incorporated in EVA at 10 wt% total loading and were compared to EVA/ATH (ATH at 65 wt% loading) and to neat EVA. The combination of AP760 and EG was made to examine whether the two types of intumescence could create additional beneficial effects and/or specific structure. The four formulations were evaluated by cone calorimetry at an external heat flux of 35 kW/m² (Fig. 2).

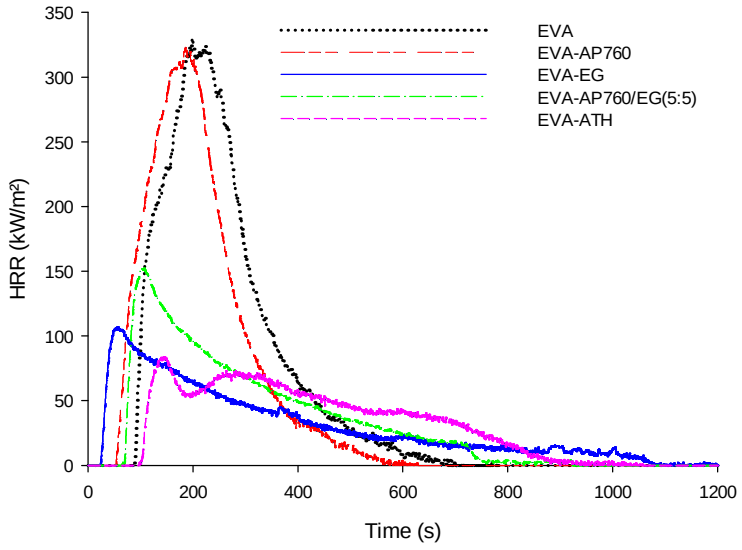

ACCEPTED MANUSCRIPT

Fig. 2. HRR curves as a function of time of intumescent EVA (external heat flux = 35 kW/m²) compared to EVA/ATH

The incorporation of AP760 does not decrease the peak of heat release rate (pHRR) compared to neat EVA and the time to ignition is shorter (20s vs. 40 s). Visually, a carbonaceous char is formed at the surface of the material but there is no expansion and the char remains flat until the flameout (Fig. 3-(a)). This poor performance can be explained by the too low loading of the intumescent FR, which cannot develop a fully expanded char protecting the material. In a previous work indeed, we showed a similar intumescent FR as AP760 provided a reduction by 80 % of pHRR when incorporated at 30 wt% in EVA [12]. On the contrary, the formulation EVA/EG exhibits a reduction by 65% of pHRR forming an expanded 'hairy' char during the experiment. The intercalation compounds contained in EG decompose rapidly into gaseous products, which blast off the graphite flakes. Those flakes make then worms forming an entangled network at the surface of the material (Fig. 3-(b)). This network acts as a protective layer. The combination of EG and AP760 in the formulation EVA-AP760/EG (5:5) provides 54% reduction of pHRR. A char exhibiting a reduced expansion is formed and some worms of graphite can be distinguished at the surface (Fig. 3-(c)). The last material to be described, namely EVA/ATH, is the basic formulation widely used to flame retard EVA in the cable and wire industry. pHRR is reduced by 70% compared to neat EVA and the time to ignition is a little bit longer. The mechanism involved is the formation of an alumina protective coating by the endothermal dehydration of ATH and water evolution (white residue of alumina containing some chunks of charred materials can be seen in Fig. 3-(d)). This type of formulation (EVA/ATH) is very efficient and it is noteworthy that similar performance can be reached with only 10 wt% EG in EVA according to the cone scenario. In all cases, a protective layer is formed at the surface of the material upon burning, protecting the substrate with different level of efficiency and hence, leading to the decrease of pHRR.

(a) EVA-AP760

(b) EVA-EG

ACCEPTED MANUSCRIPT

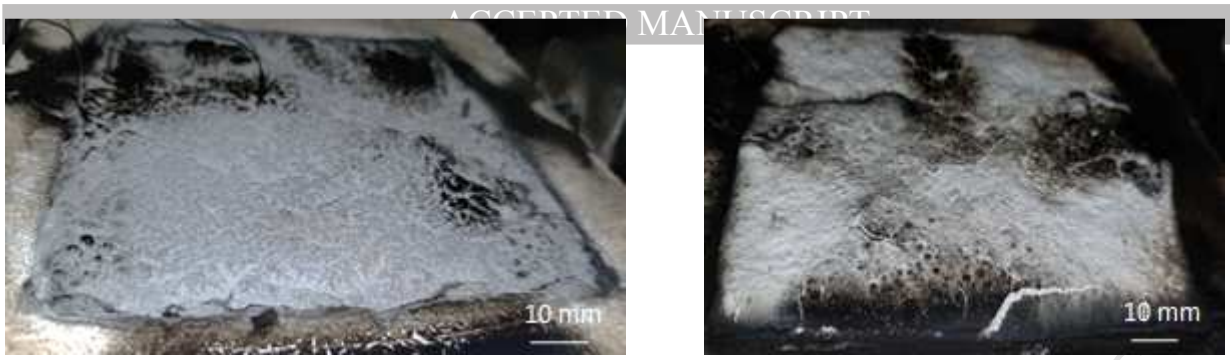

(c) EVA-AP760/EG (5:5) **(d) EVA/ATH**

Fig. 3. Cone residues of intumescent EVA ((a) to (c)) and EVA/ATH (d) (external heat flux = 35 kW/m²)

During the cone calorimetry experiments, thermocouples were placed at the backside of the materials to measure the temperature as a function of time and to quantify the efficiency of the protective barrier (thermocouple embedded in the material in horizontal position). Fig. 4 shows temperature changes as a function of time. Up to 50s, the slopes of the curves are similar and the materials heat up at about 2.4°C/s. At longer times, the curve of neat EVA does not exhibit any slope changes because it burns continuously until its complete decomposition. Note the recording was stopped when the thermocouple was no longer in the material. The formulation EVA-AP760 shows a reduction of its temperature rise between 50 and 200 s (1.3°C/s). This reduction can be assigned to the small expansion of an intumescent char. It only remains effective until 200 s evidenced by the temperature rise increasing again and becoming similar as that of neat EVA (2.4°C/s). After 285 s, the temperature drops from 540 to 500°C. This temperature drop occurs when the combustion stops: it removes the additional heat feedback of the flame and hence it decreases the total heat flux affecting the material. The temperature reaches then a pseudo-steady state at 530°C. The formation of a charred residue avoids the complete decomposition of the material and the thermocouple remains embedded in the char, permitting temperature measurement until the end of the experiment.

At t > 50s, the slopes of the intumescent EVAs (except EVA-AP760) and of EVA/ATH are much smaller than that of neat EVA. A rough estimation of the temperature rise until 600 s is 0.3°C/s. At 600 s, the temperature slope of EVA/ATH jumps to 0.6°C/s until 940 s when the temperature drops because of the flameout. The material reaches then a pseudo-steady state at 500°C. The slope break at 600s is assigned to the formation of cracks in the alumina ceramic (visual observation), leading to the release of additional flammable gases to the flame. In the case of EVA/EG and EVA-AP760/EG(5:5), the slopes' decrease compared to neat EVA corresponds to the formation of an intumescent layer reducing heat transfer from the flame to the backside of the substrate. The

ACCEPTED MANUSCRIPT

temperature curves of the two formulations are similar up to 800 s but at longer time, the slope of EVA/EG is reduced (0.2 vs. 0.3°C/s). It shows the char only formed by the entanglement of 'worms' of graphite exhibits a higher efficiency than that formed by a viscous charred layer containing worms of graphite.

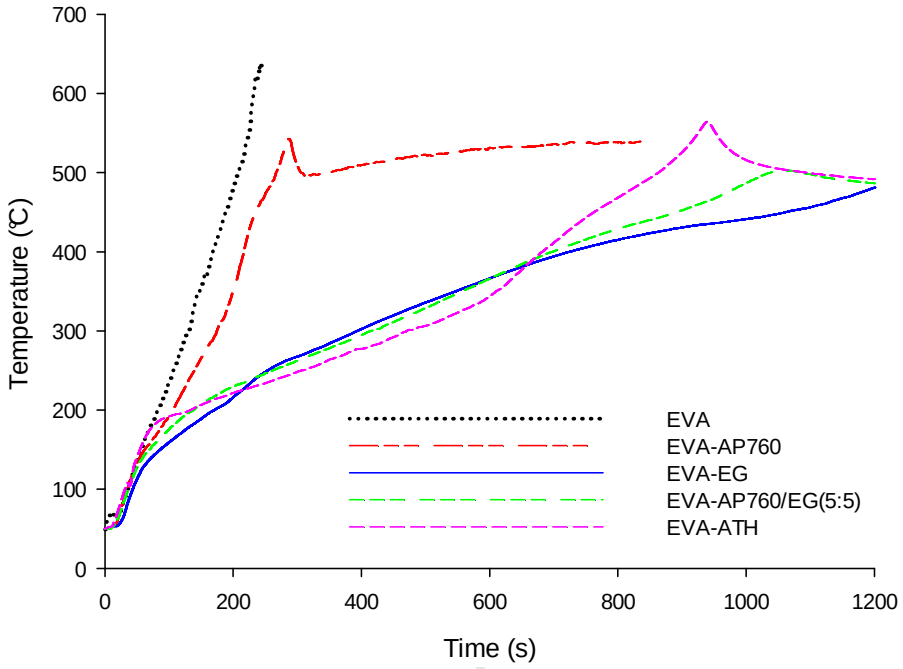

Fig. 4. Backside temperature as a function of time of EVA-based materials during cone calorimetry experiment (external heat flux = 35 kW/m²)

The results show that the FR materials form a protective barrier which can limit heat transfer from the heat source to the under layer. EVA-A760 forms a flat char at the surface, which has a limited effect for reducing the heat transfer from the flame to the material. The incorporation of EG in this formulation strongly enhances its performance. It permits the formation of a limited expanded char but exhibiting cohesiveness thanks to the graphite worms bridging the char. When the formulation contains only EG, the performance is the highest. EG forms an entangled network, which flattens because of the expansion and makes an insulative layer. It is an impressive result because EVA/EG provides a similar fire protection as EVA/ATH with a much lower loading. The high loading of ATH dilutes the combustible polymer (EVA) and forms a protective alumina layer while at low loading EG creates an efficient heat barrier.

Synergy in intumescent EVA

It was shown in the previous section AP760 does not provide high performance in EVA because of the formation of non-expanded char. The idea was to incorporate an additional ingredient acting as blowing agent in the temperature range of intumescent development (250-350°C). Zinc carbonate ($ZnCO_3$) releases high quantity of a non-flammable gas, namely CO_2, at 260°C (temperature where the mass loss rate is maximum) [13]. It is therefore a good candidate to be combined with AP760 in EVA. A series of formulations substituting 1, 2 and 5 wt% of AP760 by $ZnCO_3$ were prepared keeping the total loading constant. The formulations were evaluated by cone calorimetry and HRR curves as a function of time are depicted in Fig. 5. The incorporation of 10 wt% $ZnCO_3$ in EVA does not bring any pHRR reduction and the behavior of EVA-$ZnCO_3$ is similar as that of neat EVA. As commented in the previous section, similar conclusion can be made for EVA-AP760. The partial substitution of AP760 by $ZnCO_3$ shows a significant reduction of pHRR by 38%, 54% and 46% at 5, 2 and 1 wt% of $ZnCO_3$ respectively. The best combination is the ratio 8 to 2 (wt/wt) of AP760/$ZnCO_3$, which provides a similar performance as that obtained with the formulation EVA-AP760/EG (5:5). Note the times of ignition of all intumescent formulations are always shorter than that of the neat EVA.

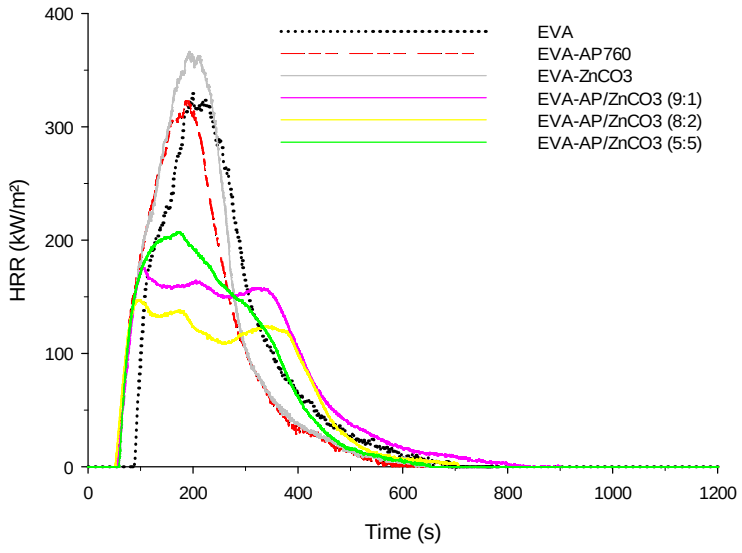

Fig. 5. HRR curves as a function of time of intumescent EVA/AP760 containing $ZnCO_3$ as synergist (external heat flux = 35 kW/m²)

The cone residues of the samples are shown in Fig. 6 (surface and cross-section of the samples). They all exhibit a similar limited expansion but the chars containing $ZnCO_3$ are less brittle than that of EVA-AP760. The cross-section of the residues does not show the formation of a foamy char as

ACCEPTED MANUSCRIPT

expected in the case of intumescent material. On the contrary, the chars are compact and packed. The surfaces of EVA-AP760/$ZnCO_3$ (5:5) and EVA-AP760/$ZnCO_3$ (8:2) contain less cracks and are smoother than those of EVA-AP760 and EVA-AP760/$ZnCO_3$ (9:1). It suggests that the addition $ZnCO_3$ brings cohesion to the intumescent char.

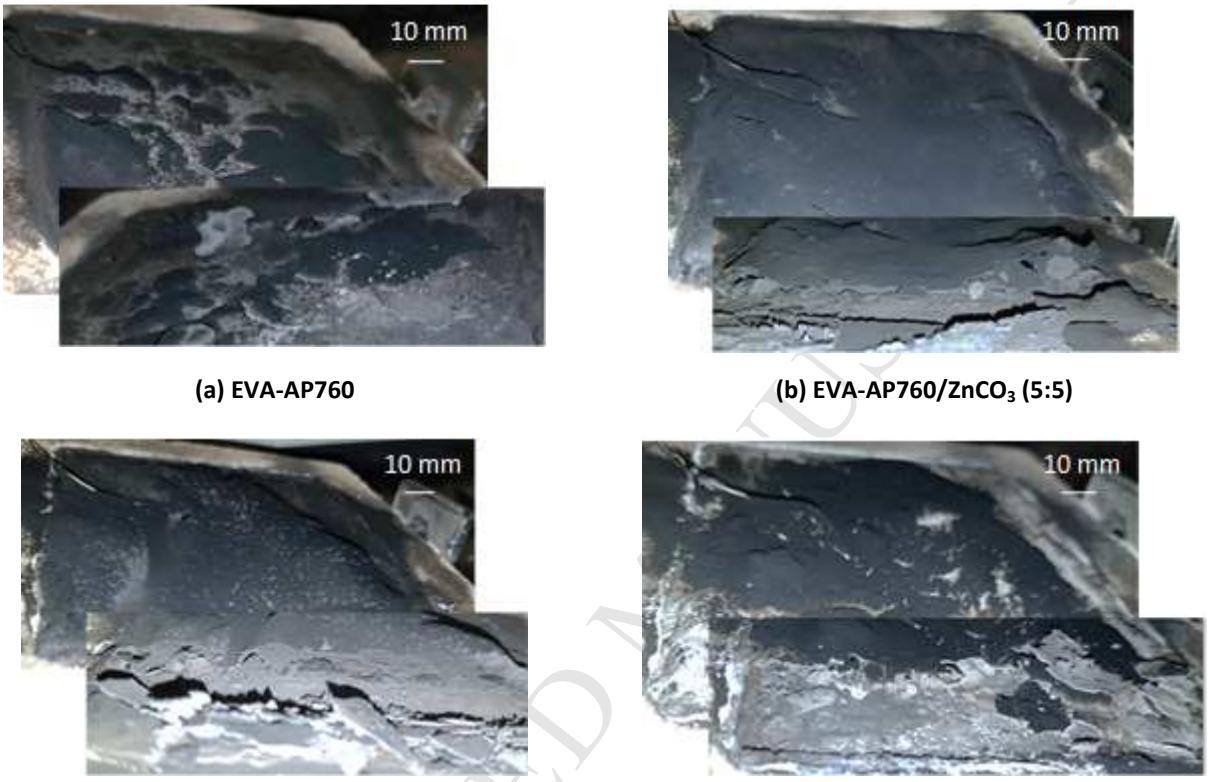

(a) EVA-AP760 **(b) EVA-AP760/$ZnCO_3$ (5:5)**

(c) EVA-AP760/$ZnCO_3$ (8:2) **(d) EVA-AP760/$ZnCO_3$ (9:1)**

Fig. 6. Cone residues of the formulation EVA-AP760/$ZnCO_3$ at different level of substitution of AP760 by $ZnCO_3$ (external heat flux = 35 kW/m²) – The pictures show the surface (up) and the cross-section (down) of the samples.

As it was done in the previous section, thermocouples were placed on the backside of the materials to measure the temperature as a function of time to quantify the efficiency of the protective barrier (Fig. 7). Up to 50s, it is observed the same behavior as the formulations EVA-AP760/EG (see Fig. 4): the slopes of the curves are similar and the materials heat up at about 2.4°C/s. The temperature curves of neat EVA and EVA-AP760 have been already commented and they are used for comparison to make comments on the effect of $ZnCO_3$. At t > 50s, the curve of EVA-AP760/$ZnCO_3$ (9:1) does not show a slope break at 200 s as in the case of EVA-AP760. The temperature rise is constant at 1.3°C/s and reaches a pseudo steady state at 530°C. The interesting feature is that the slopes of EVA-AP760/$ZnCO_3$ (8:2) and EVA-AP760/$ZnCO_3$ (5:5) are reduced compared to EVA-

ACCEPTED MANUSCRIPT

AP760/$ZnCO_3$ (9:1) (1.3 vs. 0.7°C/s) between 50 and 200s. At t > 200s, the temperature curve of EVA-AP760/$ZnCO_3$ (5:5) merges with that of EVA-AP760/$ZnCO_3$ (9:1). On the contrary, the curve of EVA-AP760/$ZnCO_3$ (8:2) does not exhibit any slope break but it keeps a constant temperature rise of 0.7°C/s until reaching its pseudo steady state after 400 s at 530°C. It evidences the formulation EVA-AP760/$ZnCO_3$ (8:2) forms a stronger char than the other formulations. The reason is not clear because the structure of the residues looks similar (see cross-section of the residues on Fig. 6) and it cannot explain the difference of behavior. It is suspected the chemical composition of the char should play a role as it was evidenced in some previous work [14-16].

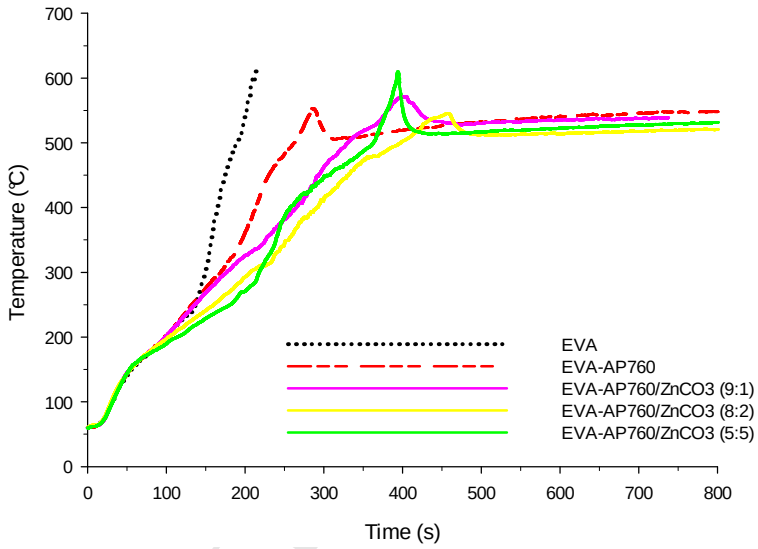

Fig. 7. Backside temperature as a function of time of EVA-AP760 materials during cone calorimetry experiment (external heat flux = 35 kW/m²)

The formation of an intumescent char is a complicated process involving several critical aspects: rheology (expansion phase, viscoelasticity of char), chemistry (charring) and thermophysics (limitation of heat and mass transfer) [17]. According to our results, $ZnCO_3$ should play a role in the chemistry of formation of the char. Solid state NMR is a powerful tool to examine the chemical composition of char and carbon 13 and phosphorus 31 are two appropriate nuclei to characterize the chars [15, 18, 19]. These chars were prepared as a function of the characteristic times of the HRR curves, namely at the ignition, at the peak of HRR and after flameout (final residue). The heat flux was shut down and the samples were taken out at the selected time. They were then characterized by CP/DD-MAS ^{13}C NMR (Fig. 8) and DD-MAS ^{31}P NMR (Fig. 10).

ACCEPTED MANUSCRIPT

The non-degraded materials (t_0) with and without $ZnCO_3$ show the same ^{13}C NMR spectra. The resonance band at 21 ppm corresponds to the CH_3- group of the acetic acid functionality of EVA [20]. The bands at 25, 30 and 35 ppm are attributed to the CH_2- groups in the polymer backbone [21]. The multiplicity of the peaks is due to several different monomer sequences in the polymeric chain because the vinyl acetate copolymerizes with ethylene and makes a random copolymer [22]. The band assigned to CH is detected at 72 ppm [20]. The chemical shift at 170 ppm corresponding to C=O in the acetate group is not observed (except a tiny band for EVA-AP760, (Fig. 8 (a)). It is probably due to experimental conditions using cross-polarization where the carbon linked to protons gives much more intense bands than that without any linked protons [23]. At the ignition (t_{ig}), the spectra of the two materials are similar. The materials were heated up and they are starting degrading by deacetylation of EVA (release of acetic acid): there is a change of the intensity ratio of the bands located at 30 and 35 ppm and formation of polyethylenic chains containing unsaturated carbons. It explains therefore the disappearance of the bands at 21 and 25 ppm and the appearance of the additional band at 130 ppm. This latter band can be also assigned to the carbonization of the material forming aromatic and/or polyaromatic species [18]. It makes sense because visual observation shows the charring of the materials. At the peak of HRR (t_{pHRR}), the same bands are observed indicating the charring of the material protecting EVA of complete decomposition. Note the low intensity of the band assigned to polyaromatic species (130 ppm) is due to the use of cross-polarization as mentioned above and so, it is not a quantitative information. The spectra of the residues are completely different: there is no signal in the case of EVA-AP760 while aliphatic species are still observed in the case of EVA-AP760/$ZnCO_3$ and the band assigned to polyaromatic species broadens. The loss of signal can be assigned to paramagnetic carbons contained in the residue [24]. The formation of large polyaromatic structure (char) is made by dehydrogenation creating radical carbons stabilized by resonance and the high number of radicals leads to the broadening of the band at 130 ppm until losing the signal. Note the presence of free radicals on aromatic carbons does not avoid the detection of aliphatic species [24] and it means those latter species are completely degraded. The main information is the addition of $ZnCO_3$ in the intumescent system permits to keep aliphatic species in the char and hence limits the decomposition of EVA.

ACCEPTED MANUSCRIPT

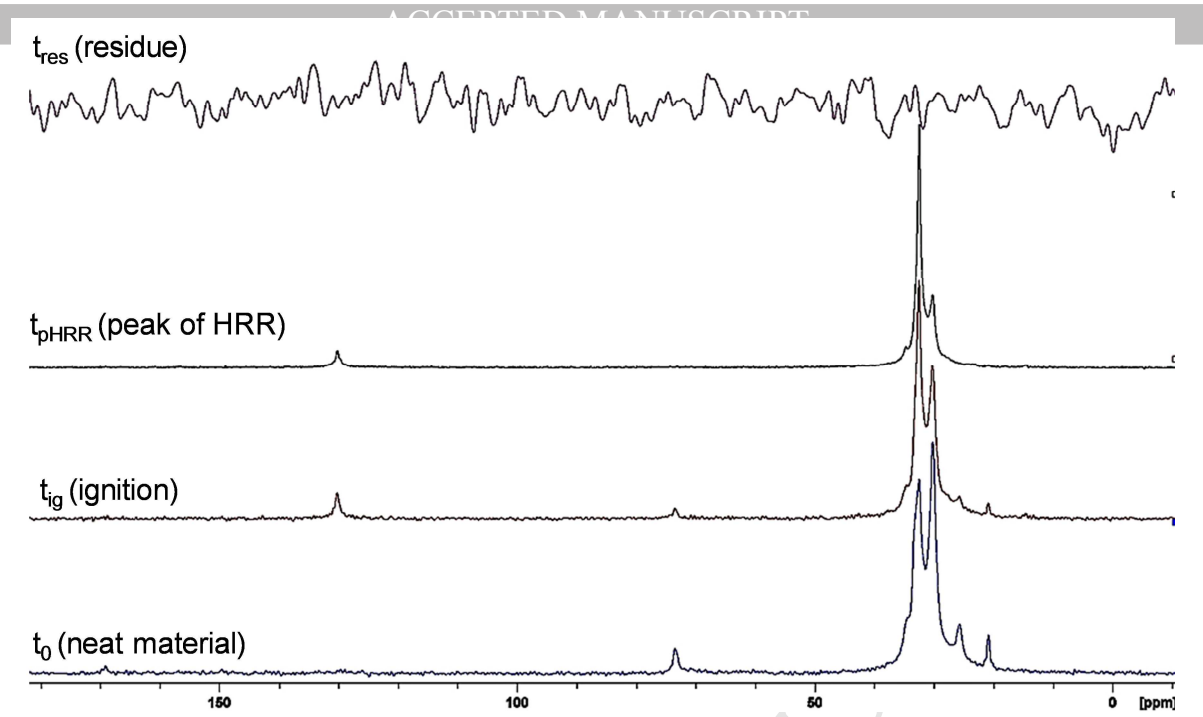

(a) EVA-AP760

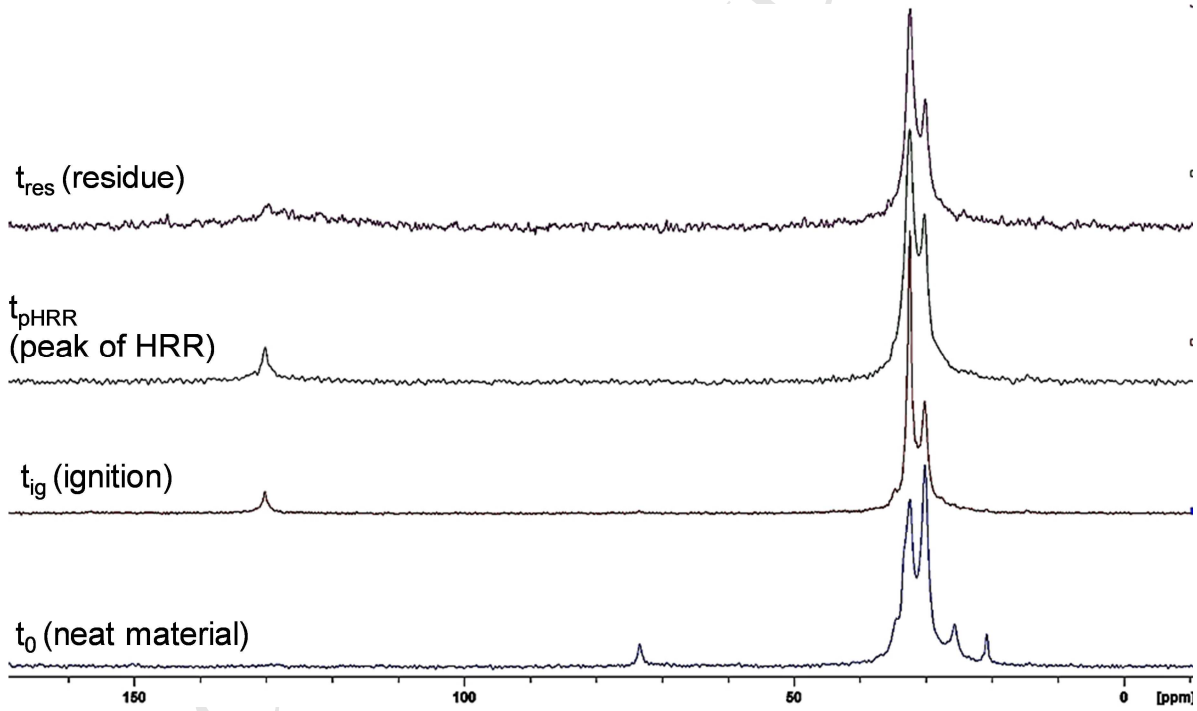

(b) EVA-AP760/$ZnCO_3$ (8:2)

Fig. 8. CP/DD-MAS ^{13}C NMR spectra as a function of cone characteristic times of (a) EVA-AP760 and (b) EVA-AP760/$ZnCO_3$ (8:2)

Ammonium polyphosphate (APP) is contained in AP760 and is one of the main ingredients of the intumescent flame retardant. Upon heating, it decomposes and yields acidic phosphates acting as char promoter [6]. They play a significant role in the charring and in the formation of an intumescent coating and the evolution of the phosphate species should be revealed by ^{31}P NMR. The same samples as above were characterized by ^{31}P NMR. Note the number of bridging oxygen

ACCEPTED MANUSCRIPT

atoms allows classifying the phosphate structure using Q^n terminology, where n represents the number of bridging oxygen atoms per phosphorus tetrahedron (Fig. 9), was used in the following [15].

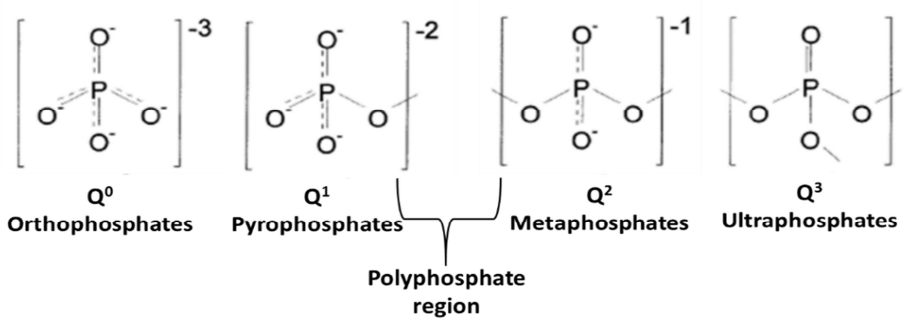

Fig. 9. Q structure of phosphate: Q^0 isolated units (ortho-P), Q^1 end units (pyro-P), Q^2 middle units (meta-P) and Q^3 crosslinking units (ultra-P)

The spectra of the neat materials (t_0) exhibit a doublet located at -22 and -24 ppm assigned to Q^2 site. This doublet is characteristic of P in APP as already reported in our previous work [25]. It is noteworthy additional bands at -26 and -27 ppm can be distinguished on the spectrum of EVA-AP760/$ZnCO_3$. They are assigned to Q^3 site probably due to the condensation (deamination and dehydration) into ultraphosphate of a low amount of APP during the processing of the formulation and/or to the formation of low amount of zinc orthophosphate [26]. At the ignition (t_{ig}), the two spectra are similar and three sharp bands located at 0, -7 and -12 ppm can be distinguished. The band at 0 ppm is assigned to Q^0 site and corresponds to orthophosphate (probably mainly phosphoric acid) [27]. The bands at -7 and -12 ppm are attributed to Q^2 sites corresponding to pyrophosphates and/or to orthophosphates linked to aromatic species (in this case, it is a Q^1 structure) [28]. Those results are consistent with the literature and they can be explained by the mechanism of decomposition of APP. When heated, APP condensates into ultraphosphate which is decomposed at higher temperature to yield orthophosphates and pyrophosphates. Those Q sites can also be embedded in the char. The behavior of the two formulations becomes different at the time when the peak of HRR occurs (t_{pHRR}). Additional broad bands of low intensity centered at -22, -28, -46 and -53 ppm can be distinguished on the spectrum of EVA/AP760. The bands at -22 and -28 ppm are assigned to Q^2 structure (ultraphosphate) [26] and those at -46 and -53 ppm to Q^3 site (highly condensed phosphate and P_2O_5 rich material) [28]. It occurs because of the condensation of phosphate due to the temperature rise in the sample. For EVA-AP760/$ZnCO_3$, it is observed an additional broad band centered at -32 ppm and lying from -22 to -40 ppm. The broadness of the

ACCEPTED MANUSCRIPT

band is explained by the formation of disordered structure of phosphates [15]. Indeed, a continuous distribution of ^{31}P isotropic chemical shifts reflects the structural disorder such as bond angle and bond length variations as well as coordination sphere disorder of the structure. This behavior can be assigned to the formation of amorphous phosphate-type exhibiting Q^3 and Q^4 sites [26]. It suggests the formation of zinc ultraphosphate glass, which is easily formed from phosphoric acid and zinc oxide. It also explains the different behavior between the formulations with and without $ZnCO_3$ and it emphasizes the role of $ZnCO_3$ in the intumescent system. In the final residues, the spectra are similar as those recorded at t_{pHRR} except for the intensities of the bands. The number of Q^0 sites decreases while the number of Q^2 and Q^3 sites increases indicating the condensation of phosphates.

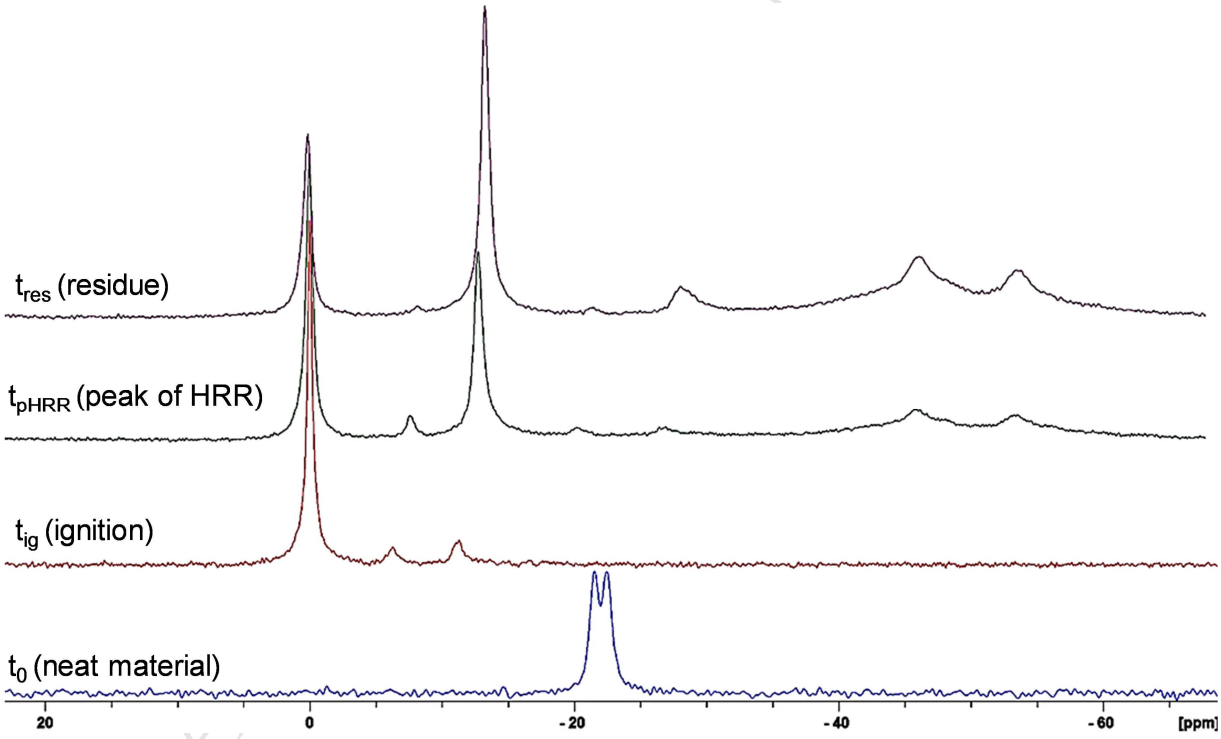

(a) EVA-AP760

ACCEPTED MANUSCRIPT

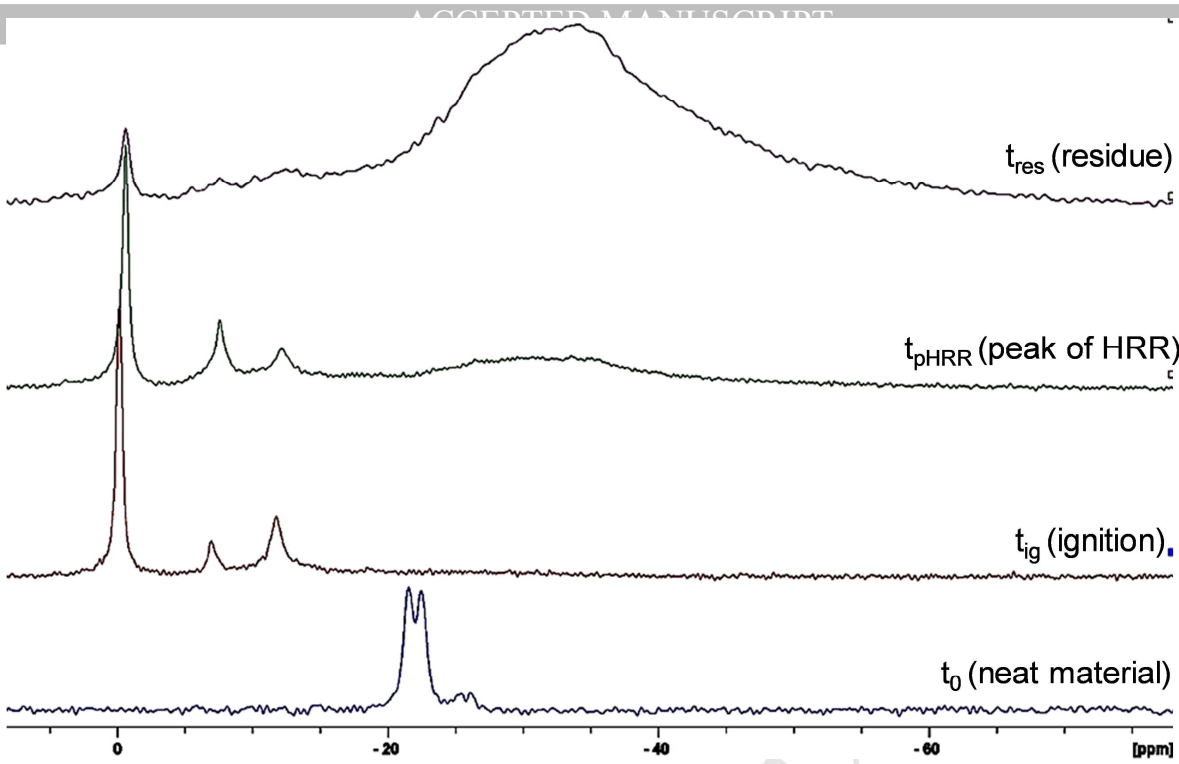

(b) EVA-AP760/$ZnCO_3$ (8:2)

Fig. 10. DD-MAS ^{31}P NMR spectra as a function of cone characteristic times of (a) EVA-AP760 and (b) EVA-AP760/$ZnCO_3$ (8:2)

NMR analyses evidence the role of $ZnCO_3$ in the formation of char. Upon heating, the two formulations decompose and yield char. The char contains phosphate species coming from the decomposition of APP, which are embedded in the charred structure. After the ignition, the temperature rises up in the char and the addition of $ZnCO_3$ permits the formation of zinc ultraphosphate glass in the char while only 'free' condensed phosphates are formed without $ZnCO_3$. It is assumed the formation of glass makes a 'glue' in the char providing a certain flexibility and resistance to the char and hence, limiting the formation of cracks (see the picture of the final residues on Fig. 6). The result is aliphatic species are 'trapped' in the char limiting the release of flammable gases to the flame. It is supported by the comparison of the mass loss rate (MLR) of EVA-AP760 and EVA-AP760/$ZnCO_3$ (8:2) (Fig. 11). MLR of EVA-AP760/$ZnCO_3$ (8:2) is much lower than that of EVA-AP760 (MLR twice lower at the maximum) evidencing lower gases flow feeding the flame over time. Hence, pHRR is strongly decreased and a synergistic effect is obtained.

ACCEPTED MANUSCRIPT

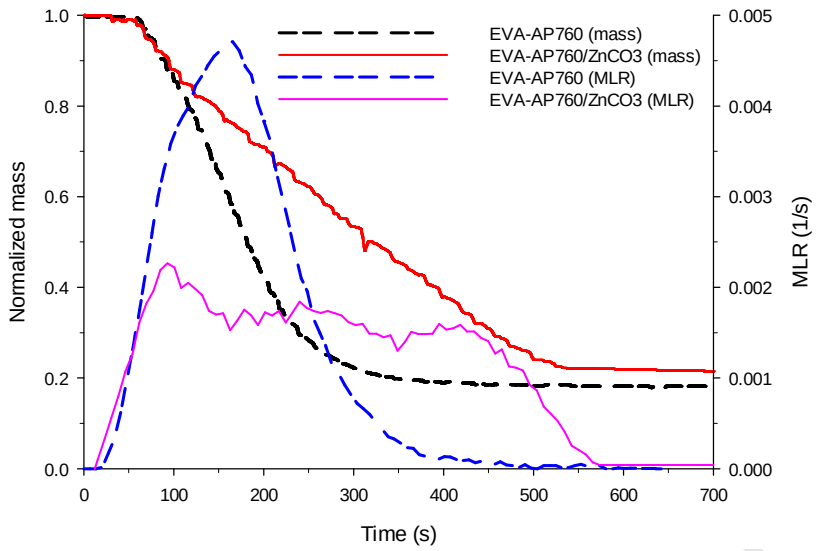

Fig. 11. Normalized mass and mass loss rate (MLR) as a function of time of EVA-AP760 and EVA-AP760/$ZnCO_3$ (8:2) measured during cone calorimetry experiment

To evidence the mechanical reinforcement of the intumescent char, its resistance was measured using a plate-plate rheometer. The force of the upper plate as a function of the gap between the two plates is plotted on Fig. 12. It shows the char made from EVA-AP760 is relatively fragile since low force applied on it is enough to crash it down (see the gap between 4 and 1.5 mm). The force rise then up because the char is compacted between the plates. On the opposite, the force to apply on the char of EVA-AP760/$ZnCO_3$ (8:2) is higher (see the gap between 3.5 and 1.8 mm) evidencing the role of $ZnCO_3$ as mechanical reinforcer.

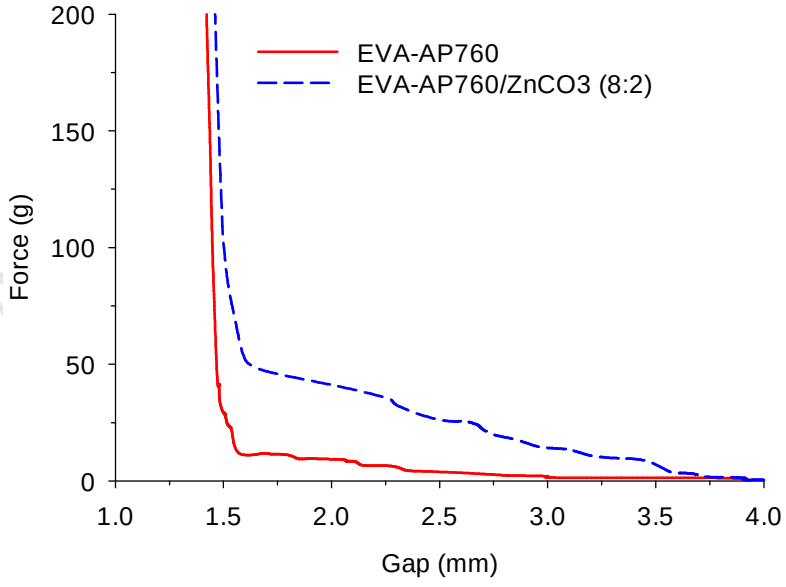

Fig. 12. Measurement of the mechanical resistance of the two intumescent chars (EVA-AP760 and EVA-AP760/$ZnCO_3$ (8:2))

CONCLUSION

In this work, two types of intumescence (physical and chemical expansion) were evaluated to make flame retarded EVA. The incorporation of EG (physical expansion) at relatively low loading (10 wt%) in EVA permits the reduction up to 65% of pHRR in formulations containing EG while the reduction is not significant with the same loading of AP760 (chemical expansion). EVA-AP760 makes a flat char not able to limit heat transfer while EVA-EG forms an entangled network of graphite worm acting as heat barrier.

The incorporation of small amount of $ZnCO_3$ in EVA-AP760 enhances strongly the performance: the pHRR was not reduced only with AP760 while it is decreased by 54% when 2 wt% of AP760 is substituted by $ZnCO_3$. It evidences a strong synergistic effect between AP760 and $ZnCO_3$. The mechanism was elucidated characterizing by solid state NMR of ^{13}C and ^{31}P residues prepared at different characteristic times of HRR curves. It was shown that the protective char is reinforced by the formation of phosphate glass limiting the creation of cracks and increasing the char strength. Aliphatic species are also 'trapped' in the char limiting the release of flammable gases to the flame. The addition of low cost additional filler (ZnCO3) to an intumescent system offers the benefit to make high effective FR intumescent system at low loading for EVA.

ACKNOWLEDGEMENT

This work has received funding from the European Research Council (ERC) under the European Union's H2020 – the Framework programme for Research and Innovation (2014-2020) / ERC Grant Agreement n°670747 – ERC 2014 AdG/FireBar-Concept.

REFERENCES

[1] M.K. Mishra, Y. Yagci, Handbook of Vinyl Polymers: Radical Polymerization, Process, and Technology: Second Edition, CRC Press2016.
[2] A. Witkowski, A.A. Stec, T.R. Hull, The influence of metal hydroxide fire retardants and nanoclay on the thermal decomposition of EVA, Polym. Degrad. Stab. 97(11) (2012) 2231-2240.
[3] L.P. Dong, C. Deng, R.M. Li, Z.J. Cao, L. Lin, L. Chen, Y.Z. Wang, Poly(piperazinyl phosphamide): A novel highly-efficient charring agent for an EVA/APP intumescent flame retardant system, RSC Advances 6(36) (2016) 30436-30444.
[4] C. Feng, M. Liang, J. Jiang, H. Liu, J. Huang, Synergistic effect of ammonium polyphosphate and triazine-based charring agent on the flame retardancy and combustion behavior of ethylene-vinyl acetate copolymer, J. Anal. Appl. Pyrolysis 119 (2016) 259-269.
[5] T. Giang, D. Hoang, J. Kim, Effect of intumescent compositions on flammable properties of ethylene vinyl acetate and polypropylene, Fire Mater. 41(7) (2017) 857-863.

ACCEPTED MANUSCRIPT
[6] J. Alongi, Z. Han, S. Bourbigot, Intumescence: Tradition versus novelty. A comprehensive review, Prog. Polym. Sci. 51 (2015) 28-73.
[7] S. Duquesne, R. Delobel, M. Le Bras, G. Camino, A comparative study of the mechanism of action of ammonium polyphosphate and expandable graphite in polyurethane, Polym. Degrad. Stab. 77(2) (2002) 333-344.
[8] Y. Lu, Y. Zhang, W. Xu, Flame retardancy and mechanical properties of ethylene-vinyl acetate rubber with expandable graphite/ammonium polyphosphate/dipentaerythritol system, J. Macromol. Sci., Part B: Phys. 50(10) (2011) 1864-1872.
[9] C. Guo, L. Zhou, J. Lv, Effects of expandable graphite and modified ammonium polyphosphate on the flame-retardant and mechanical properties of wood flour-polypropylene composites, Polymers and Polymer Composites 21(7) (2013) 449-456.
[10] W.W. Focke, H. Badenhorst, W. Mhike, H.J. Kruger, D. Lombaard, Characterization of commercial expandable graphite fire retardants, Thermochim. Acta 584 (2014) 8-16.
[11] M. Jimenez, S. Duquesne, S. Bourbigot, Characterization of the performance of an intumescent fire protective coating, Surf. Coat. Technol. 201(3-4) (2006) 979-987.
[12] M. Bugajny, S. Bourbigot, M. Le Bras, R. Delobel, The origin and nature of flame retardance in ethylene-vinyl acetate copolymers containing hostaflam AP 750, Polym. Int. 48(4) (1999) 264-270.
[13] F.J. Gotor, M. Macías, A. Ortega, J.M. Criado, Simultaneous use of isothermal, nonisothermal, and constant rate thermal analysis (CRTA) for discerning the kinetics of the thermal dissociation of smithsonite, Int. J. Chem. Kinet. 30(9) (1998) 647-655.
[14] S.P.D.S. Ribeiro, L.D.S. Cescon, R.Q.C.R. Ribeiro, A. Landesmann, L.R.D.M. Estevão, R.S.V. Nascimento, Effect of clay minerals structure on the polymer flame retardancy intumescent process, Appl. Clay Sci. 161 (2018) 301-309.
[15] N. Hansupo, G. Tricot, S. Bellayer, P. Roussel, F. Samyn, S. Duquesne, M. Jimenez, M. Hollman, P. Catala, S. Bourbigot, Getting a better insight into the chemistry of decomposition of complex flame retarded formulation: New insights using solid state NMR, Polym. Degrad. Stab. 153 (2018) 145-154.
[16] S. Pappalardo, P. Russo, D. Acierno, S. Rabe, B. Schartel, The synergistic effect of organically modified sepiolite in intumescent flame retardant polypropylene, Eur. Polym. J. 76 (2016) 196-207.
[17] C. Gérard, G. Fontaine, S. Bellayer, S. Bourbigot, Reaction to fire of an intumescent epoxy resin: Protection mechanisms and synergy, Polym. Degrad. Stab. 97(8) (2012) 1366-1386.
[18] A. Karrasch, E. Wawrzyn, B. Schartel, C. Jäger, Solid-state NMR on thermal and fire residues of bisphenol A polycarbonate/silicone acrylate rubber/bisphenol A bis(diphenyl-phosphate)/(PC/ SiR/BDP) and PC/SiR/BDP/zinc borate (PC/SiR/BDP/ZnB) - Part I: PC charring and the impact of BDP and ZnB, Polym. Degrad. Stab. 95(12) (2010) 2525-2533.
[19] A. Karrasch, E. Wawrzyn, B. Schartel, C. Jäger, Solid-state NMR on thermal and fire residues of bisphenol A polycarbonate/silicone acrylate rubber/bisphenol A Bis(diphenyl-phosphate) (PC/SiR/BDP) and PC/SiR/BDP/zinc borate (PC/SiR/BDP/ZnB) - Part II: The influence of SiR, Polym. Degrad. Stab. 95(12) (2010) 2534-2540.
[20] N. Pécoul, S. Bourbigot, B. Revel, 13C, 25Mg and 11B solid-state NMR study of a fire retarded ethylene-vinyl acetate copolymer, Macromol. Symp. 119 (1997) 309-315.
[21] G.C. Stael, M.I.B. Tavares, NMR carbon-13 high resolution study of poly(ethylene-co-vinyl acetate), Polym. Test. 16(2) (1997) 193-198.
[22] M. Delfini, A.L. Segre, F. Conti, Sequence Distributions in Ethylene–Vinyl Acetate Copolymers. I.13C Nuclear Magnetic Resonance Studies, Macromolecules 6(3) (1973) 456-459.
[23] S. Bourbigot, M.L. Bras, R. Delobel, Carbonization mechanisms resulting from intumescence association with the ammonium polyphosphate-pentaerythritol fire retardant system, Carbon 31(8) (1993) 1219-1230.
[24] S. Bourbigot, M. Le Bras, R. Delobel, J.M. Trémillon, Synergistic effect of zeolite in an intumescence process: Study of the interactions between the polymer and the additives, Journal of the Chemical Society - Faraday Transactions 92(18) (1996) 3435-3444.
[25] F. Samyn, S. Bourbigot, S. Duquesne, R. Delobel, Effect of zinc borate on the thermal degradation of ammonium polyphosphate, Thermochim. Acta 456(2) (2007) 134-144.
[26] C. Mercier, L. Montagne, H. Sfihi, G. Palavit, J.C. Boivin, A.P. Legrand, Local structure of zinc ultraphosphate glasses containing large amount of hydroxyl groups: 31P and 1H solid state nuclear magnetic resonance investigation, J. Non-Cryst. Solids 224(2) (1998) 163-172.
[27] A. Sut, S. Greiser, C. Jäger, B. Schartel, Synergy in flame-retarded epoxy resin: Identification of chemical interactions by solid-state NMR, J. Therm. Anal. Calorim. 128(1) (2017) 141-153.
[28] S. Bourbigot, M. Le Bras, R. Delobel, R. Decressain, J.P. Amoureux, Synergistic effect of zeolite in an intumescence process: Study of the carbonaceous structures using solid-state NMR, Journal of the Chemical Society - Faraday Transactions 92(1) (1996) 149-158.

Two types of intumescence: physical and chemical expansion

Low loading of expandable graphite provides lower pHRR (lower than that of EVA/ATH at 65 wt%)

Zinc carbonate is a superior synergist for conventional intumescent EVA (chemical expansion)

Zinc carbonate: reinforcement of the protective char by the formation of phosphate glass

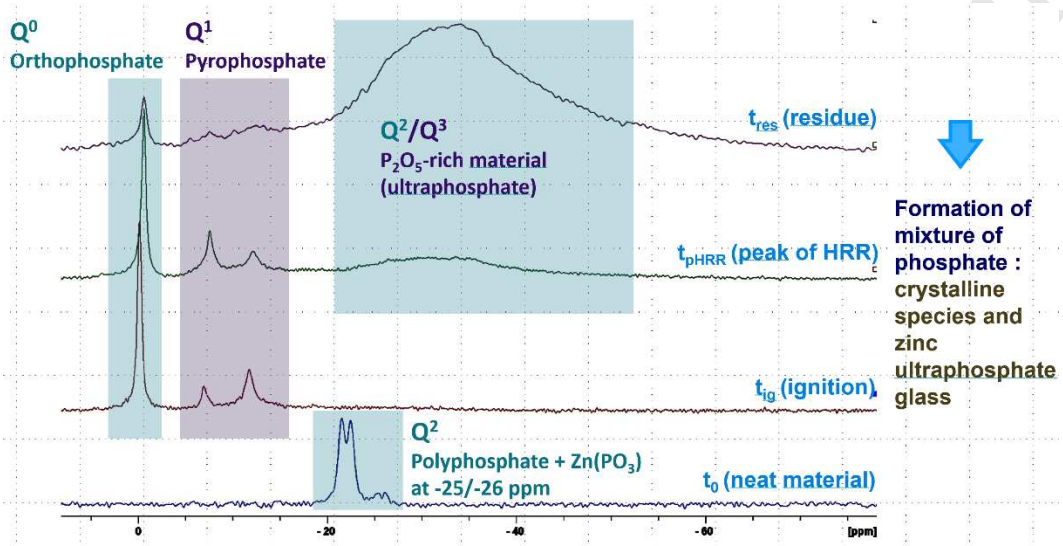

ACCEPTED MANUSCRIPT